FACADE RENOVATION FOR A PUBLIC BUILDING BASED ON A WHOLE-LIFE VALUE APPROACH

Qian Jin[1], Mauro Overend[1]
[1]Department of Engineering, University of Cambridge, Cambridge, UK

ABSTRACT

Façade design is a complex design and optimisation process. One of the difficulties is to understand how an existing building performs in the real world, which is essential to ensure the reliability of the building performance simulation used during façade design process. Another challenge is to devise a façade design option that represents the optimal trade-offs among different design objectives.

This paper presents the use of a recently developed whole-life value based façade design and optimisation tool on a real-world façade renovation project. It illustrates the process of identifying the optimised façade. The principal outcome of the paper is a series of optimal façade solutions that improve the social, environmental and economic value of the building at a reasonable capital economic cost. The building performance simulation is validated by in-situ measurements. The whole-life value based design approach produces optimal trade-offs between different design objectives and improves the quality of early stage design decisions.

INTRODUCTION

Building energy simulation and optimisation techniques are often used during the façade design process. They provide quick and quantitative analysis to assist decision-making. However, two major barriers to devise the optimal façade design still exist. Firstly, the credibility gap exists, i.e., the computational simulation results are only as reliable as the model itself, and it is often difficult to know how far the deviation from the real-world situation is. A second challenge is to devise an optimal façade solution by evaluating the true values of alternative façade designs. A commonly used selection approach is to decompose the design criteria into their respective disciplines (e.g., structural, environmental, etc), which can then be evaluated through mono-disciplinary commercial software. This approach however overlooks the dynamic interaction between the cross-disciplinary design criteria.

This paper describes the implementation of building simulation and optimisation in a building envelope renovation project. In-situ measurement is carried out to provide the basis for validating a building energy simulation model, which will be used for subsequent design analysis. Five rennovation strategies are proposed, and a preliminary investigation is performed to understand the performance improvement potential of each strategy. Finally, a whole-life value based multi-objective optimisation approach is deployed to devise the optimal façade in terms of the three design objective values: social, economic, and environmental. The social value is evaluated using an 'ambient-performance' relationship (Jin *et al.,* 2011) that converts indoor environment quality (thermal comfort, visual comfort, aural comfort, and air quality) to occupant productivity. The economic value is evaluated by the cash payback period through whole-life costing approach. The environmental value is evaluated by the carbon payback period through life-cycle analysis. The evaluation of the three objective values is performed using 3rd party software and specially developed MATLAB scripts. Optimal façade design options that strike the trade-offs between the three design objectives are proposed.

SIMULATION AND EXPERIMENT

Project description

The Inglis Building is part of the Department of Engineering, University of Cambridge and was constructed in 1945. It is a five-story steel-framed building with reinforced concrete floors. It adopts mixed-mode ventilation. The buliding has a gas-fired central heating system that consists of low-temperature hot water radiators. The façade earmarked for refurbishment is facing north and encompasses the mezzanine floor, the first and the second floor. It was constructed in 1964. It consists of single glazing with thermally unbroken aluminium frames and brickwork spandrels. The objective of this study is to propose an optimal façade solution that (i) reduces the carbon emission of the building; (ii) is economically viable; (iii) improves occupant comfort.

In-situ measurement

Since the building was built almost 70 years ago, current knowledge about the building service system such as capacity and control strategy was insufficient for building energy simulation. Therefore, in-situ measurement was carried out to capture relevant

data. The data obtained was then used in the numerical simulation either as input or as a means of validation.

A north facing office room A the Mezzanine floor (Figure 1) was monitored during Dec 21st 2011 to Dec 27th 2012. It was unoccupied during the testing period, and the windows were closed all the time. The dry bulb temperature in the middle of the room, the radiator surface temperature in the room, and the dry bulb temperature in the corridor space adjacent to the offices (temperature sensor was located at Location B in Figure 1 were recorded at an interval of 10 minutes by wireless temperature sensors with an accuracy of ±0.5°C. Meanwhile, the outdoor dry bulb temperature, relative humidity, and dew point temperature were measured using the same temperature sensors; the outdoor atmospheric pressure, wind speed, and wind direction was obtained from the Cambridge Weather Station (DTG, 2012). The dry bulb temperatures obtained are shown in Figure 2.
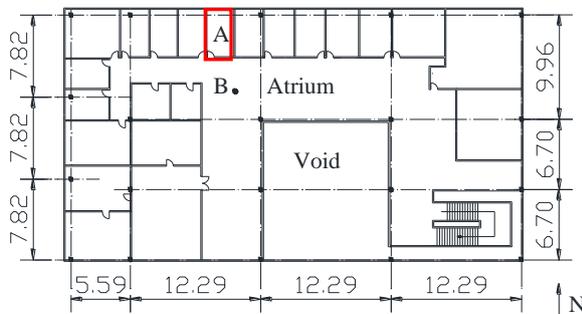

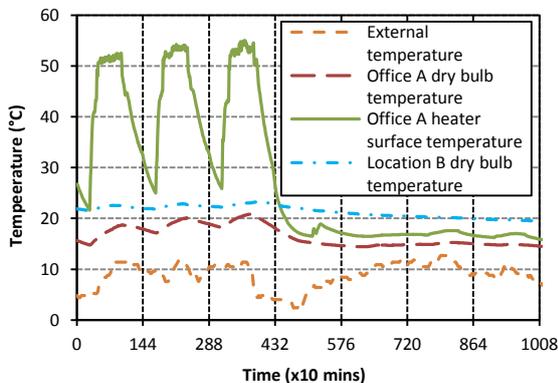*Figure 1 Mezzanine floor plan view (Unit: m).*

Figure 2 External dry bulb temperature, dry bulb temperature in Office A and Location B, and radiator surface temperature in Office A.

An infiltration test was carried out in Office A resulting in 10.32ac/h at 50 Pa, which is equivalent to an average annual infiltration rate of 0.47ac/h (CIBSE, 2006).

The office was heated by a low-temperature hot water radiator in the first three days and unheated for the last four days. The maximum flow rate going through the radiator was measured using an ultrasound electronic device Portaflow 330 (Micronics Ltd, 2010), with an accuracy ±6% The

device consists of a pair of ultrasonic transmitters / receivers. It measures the flow rate by comparing the speed of the signal transmitted upstream with that transmitted downstream (Figure 3). Figure 4 shows how the transducers were mounted to the pipe being measured. The heating system was adjusted to run at the highest capacity on the testing day. The maximum flow rate obtained is 0.032 L/s.
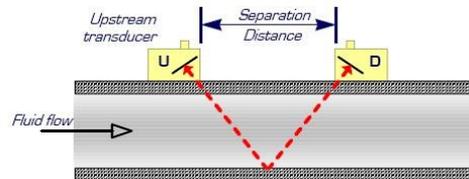

Figure 3 Principles of operation (Ltd 2010).

Figure 4 Transducer mounting.

There are some tall trees to the north of the Inglis building, which provide shading for the north facade. Since they are modelled as external shading for the north façade. It is assumed that the shading effect for solar heat is the same with that for visible daylight. Therefore, the light illuminance on the facade of the Mezzanine floor (shaded by the trees) and that of the 2nd floor (high enough to avoid the shading) were measured using a digital lux meter with an accuracy of ±5%. The measurements are carried out on Oct 9, 2011 and Mar 12, 2012. It was overcast on both dates to ensure the daylight was diffused. The transmittance of the trees measured on the two days are taken as the average transmittance during summer (Jun 1 – Oct 30) and winter (Nov 1 – May 31), which are 0.75 and 0.86, respectively.

Simulation

- Computational model validation

The first part of the simulation involves modelling Office A using the data obtained from the in-situ measurement. The objective is to validate the computational model by comparing the simulated result with the experimental data. The geometry of Office A is 4.6 m (depth) x 3.4 m (width) x 3.3 m (height). The section through the north facade is shown in Figure 5. The floor and ceiling consist of 280 mm concrete slat and 22.5 mm raised timber floor with a 54 mm air gap in between. The partition walls consist of 100 mm brick faced with 19 mm gypsum boards on both sides.

A building energy simulation software EnergyPlus 7.0 (LBNL, 2011) is used in this study. The load convergence tolerance value in the numerical model was set to 0.04, and the temperature convergence tolerance value was set to 0.01. The time step is set to

10 minutes. Beam solar radiation is assumed to be distributed on each surface of the room. The interior convection model correlates the heat transfer coefficient to surface orientation and temperature difference between the surface and the room air. The exterior convection model calculates heat transfer coefficients from roughness, wind speed, and the site's terrain.
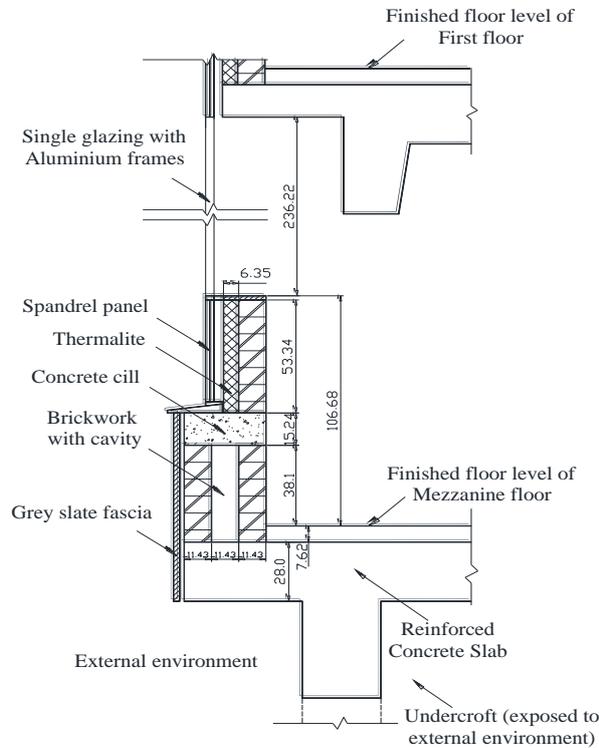

Figure 5 Cross section of the façade for the Mezzanine floor. (Unit: cm)

The partition walls that separate Office A from other office rooms were assumed adiabatic. The floor is exposed to external environment, and the ceiling is assumed adiabatic. Since the dry bulb temperature in Location B is higher and less volatile than that in Office A (Figure 2), there is heat transfer through the partition wall between the office and the atrium. Therefore, an extended thermal zone was created adjacent to Office A, as shown in Figure 6. For this extended thermal zone, apart from its common surface with Office A and the south surface (exposed to external environment but sheltered from sun), all other surfaces are assumed adiabatic. The internal heat gain of the extended thermal zone was adjusted so that the simulated dry bulb temperature matches with that measured at Location B. This provides an accurate boundary condition for the south surface of Office A.

In Office A, the only source of internal heat gain was a PC which was kept on all the time with a design level of 110 W (Duska *et al.*, 2007). An internal thermal mass, which is equivalent to of 3m^3 wood (specific heat capacity = 1630 J/kg·K), was introduced to account for the thermal mass of the furniture and books in Office A. The rated average

water temperature, rated water mass flow rate, and rated capacity of the radiator were assumed to be 72.4°C, 0.063kg/s, and 2400 W, respectively. The radiant/convective split of the radiator is 30/70.
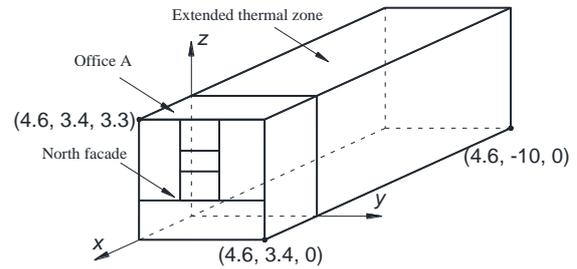

Figure 6 Numerical model of Office A. (Unit: m)

The façade consists of 4 mm thick single glazing units with a thermally unbroken aluminium frame. The U-value of the frame is 10.90 W/m^{2}K for fixed frame and 13.51 W/m^{2}K for operable frame (ASHRAE, 2009). The weather data, the radiator surface temperature, the infiltration rate, and the maximum flow rate in the radiator recorded in the in-situ measurement were used as inputs to the simulation model. The hourly water temperature profile in the radiator was established by adding 19.7°C to the hourly average temperature during the first three days in Figure 2, as shown in Figure 7. This is the temperature difference between the highest surface temperature of the radiator 72.4°C when the heating system is fully on, and the highest hourly average temperature for the first three days in Figure 2. This adjustment was made based on the assumption that the heating system will always run at full capacity, and that the occupants will manually adjust the local flow rate according to the thermal condition in their offices.
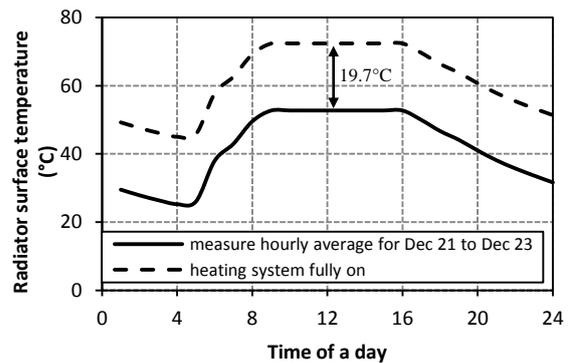
Figure 7 Measured average hourly radiator surface temperature and the temperature assumption for heating system fully on.

The global solar radiation and diffuse horizontal radiation were not monitored during the testing period, so this data was obtained from the ASHRAE International Weather for Energy Calculations (IWEC) data for Gatwick, London (ASHRAE, 2012).

The simulated dry bulb temperatures in Office A and at Location B are compared with that obtained from field measurements.

- Preliminary investigation

Five renovation strategies are proposed based on practical experience. A preliminary investigation is performed to understand the improvement potential of each strategy. The validated computational model in the previous section is implemented to evaluate: (i) the carbon payback period PB_{carbon}, (ii) cash payback period time PB_{cash}, and (iii) occupant productivity of the five strategies described as follows:

S_O: Original design without any change.

S_W: Add insulated plaster board to the internal side of the opaque external wall. A variation of Kingspan Kooltherm K17 insulated dry-lining boards is used. This consists of 12.5mm plasterboard and 40mm CFC/HCFC-free rigid phenolic insulation board. The thermal resistance is $2.2m^2$K/W. The price is £58.21 per board (2.4m x1.2m) including VAT (Kingspan, 2012). The average U-value of the opaque wall is therefore reduced from the current 1.18 W/m^2K to 0.35 W/m^2K to satisfy the Building Regulations 2010 Part L2A (DC LG, 2010).

S_G: Replace the single glazing (U-value = 5.75 W/m^2K; g-value = 82.7%; visible transmittance V_t = 90%) with double glazing (4mm glass + 16mm argon cavity + 4mm glass) with low-e coating on Surface 2 (U-value = 1.1 W/m^2K; g-value = 62%; V_t = 80%).

S_Fr: Replace existing aluminium façade frame with thermally broken aluminium one. A frame product Schuco USC 65, which has a U-value of 2.8W/m^2K, was implemented (Schuco, 2012). The frame cross-section is shown in Figure 8.

S_Fl: Add insulated plaster board to the underside of the concrete slab. A variation of Kingspan Kooltherm K17 (Kingspan, 2012) insulated dry-lining boards is used. It consists of 12.5mm plasterboard and 65mm CFC/HCFC-free rigid phenolic insulation board. The thermal resistance is $3.15m^2$K/W. The price is £60.92 per board (2.4m x1.2m) including VAT. The average U-value of the floor is reduced from 1.1 W/m^2K to 0.24 W/m^2K to satisfy the minimal requirement of 0.25 W/m^2K in Building Regulations 2010 Part L2A (DC LG, 2010).
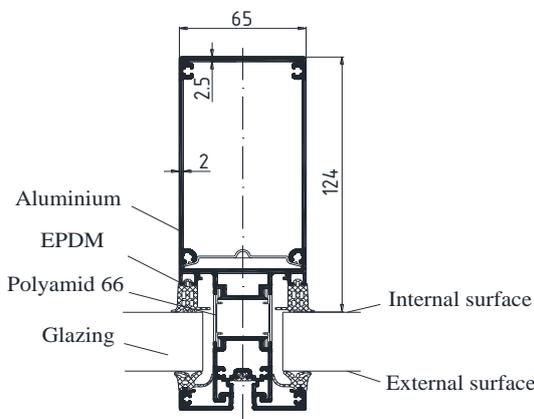

Figure 8 Cross-section of Schuco USC 65 aluminium frame with thermal break (Schuco, 2012).

PB_{carbon} is calculated from:

$$PB_{carbon} = \frac{\text{Embodied carbon of proposed materials}}{\text{Carbon saved from reduced energy demand}} \quad (1)$$

The total green house gas emissions from natural gas is 0.20155 kg CO_2 equivalent per kWh; the total green house gas emissions from electricity is 0.59368 kg CO_2 equivalent per kWh (AEA Ltd, 2011). The embordied carbon for producing different façade materials and products was calculated according to Table 1 (Kellenberger et al., 2008) and (Hammond and Jones, 2008).

Table 1 The embodied carbon and density for producing different façade materials and products (Kellenberger et al., 2008) and (Hammond and Jones, 2008).

Materials	Embodied carbon (kg CO_2 eq/kg)	DENSITY (kg/m^3)
Glazing uncoated	0.971	2500
Glazing coated	1.13	2500
Extruded aluminium	11.2	2700
EPDM	4.02	134
Polyamide 66	6.5	1140
Plasterboard	0.38	800
Brick	0.22	1922
Rigid Phenol	5.7	110

PB_{cash} is calculated from:

$$PB_{cash} = \frac{\text{Initial capital cost of proposed materials}}{\text{Energy cost saved from reduced energy demand}} \quad (2)$$

The initial capital cost of glazing is obtained by means of the indicative cost range in Table 2. The costs of gas and electricity are £0.034/kWh and £0.085/kWh, respectively. The cost of frames are unknown and therefore not considered. The labour cost for insulating is assumed to be £18/m^2.

Table 2 Indicative cost data for double and triple glazing for UK application (Thompson, 2011).

GLAZING TYPES		INDICATIVE COST (£/m^2)	MEAN (£/m^2)
Double glazing unit	Clear	125-135	130
	Clear with low-e coating	135-150	142.5
	Clear with high performance solar control and low-e coating	175-200	187.5
Triple glazing unit	Clear	180-195	187.5
	Clear with low-e coating	195-215	205
	Clear with high performance solar control and low-e coating	235-255	245

The occupant comfort is evaluated by the indoor environment quality (IEQ) cost C_{IEQ} due to occupant productivity-loss. This was calculated using the 'multi-variant IEQ - productivity' relationship (Jin *et al.*, 2012), which is summarised as follows:

Firstly, the indoor environment acceptance IEA was calculated from Eq (3) – Eq (8).

$$IEA = 1 - \frac{1}{1 + \exp[k_0 + \sum_{i=0}^{4} k_i \varphi_i(\zeta_i)]} \quad (3)$$

where φ_1 to φ_4 are the acceptance indices of thermal comfort, air quality, aural comfort and light level.

$$k_i = \begin{cases} -15.02 \\ 6.09 \\ 4.88 \\ 4.74 \\ 3.70 \end{cases} ; i = 0,...,4. \quad (4)$$

where k_1 to k_4 represent the relative importance of the four factors. φ_1 to φ_4 are calculated from Eq (3) to Eq (6) as follows:

$$\varphi_1 = 1 - \frac{PPD}{100} \quad (5)$$

where *PPD* is the predicted percentage of dissatisfied. For the *PPD* calculation, the metabolic rate is 1.2 met for office work (CIBSE, 2006). It is assumed that the work efficiency of the human body for office work is zero, i.e., all the energy produced in the body is converted to heat and none is converted to mechanical energy. The air velocity is assumed to be 0.05m/s. The clothes level is assumed to be 0.7 for summer (May - Sep) 0.85 for winter (Jan – Apr, Oct - Dec).

$$\varphi_2 = 1 - \frac{1}{2}[\frac{1}{1 + \exp(3.118 - 0.00215\zeta_2)}$$
$$- \frac{1}{1 + \exp(3.230 - 0.00117\zeta_2)}]; (500 \le \zeta_2 \le 1800) \quad (6)$$

where ζ_2 denotes the CO_2 concentration (ppm);

$$\varphi_3 = 1 - \frac{1}{1 + \exp(9.540 - 0.134\zeta_3)}; (45 \le \zeta_2 \le 72) \quad (7)$$

where ζ_3 denotes the equivalent noise level (dBA);

$$\varphi_4 = 1 - \frac{1}{1 + \exp(-1.017 + 0.00558\zeta_4)};$$
$$(200 \le \zeta_4 \le 1600) \quad (8)$$

where ζ_4 denotes the illumination (lux) at working plane.

Secondly, *IEA* is converted to indoor environment satisfaction (*IES*) using Eq (9):

$$IEA = 0.95 \exp\{-0.0312 \exp[1.7568(1-IES)]\} \quad (9)$$

Finally, the occupant productivity *OP* was related to *IES* using Eq (10):

$$OP = 15.097 \cdot IES + 75.466 \quad (-1 \le IES \le 1) \quad (10)$$

It is assumed that the salary of the occupant is £50,000. Given that there are 252 working days in a year and 8 working hours in a day. The average hourly employment cost is therefore £25/occupant. C_{IEQ} due to occupant productivity-loss for a particular façade design can therefore be calculated from Eq (11):

$$C_{IEQ} = \sum_{h=0}^{h=8760} (\frac{\text{Maximum occupant productivity}}{OP_h} - 1) \times £25 \times w_h \quad (11)$$

where h is the number of hours in a year, OP_h is the occupant productivity in during Hour h, and w_h is the weight of the occupancy during Hour h.

The annual weather data in London was used. It was assumed that the efficiency of the heating system is 100%.

The electric equipment in Office A includes a PC that with a design level of 110 W, and a PC monitor with a design level of 50W (Duska *et al.* 2007). The light level is assumed to be 58W/m^2, and is binary (either on or off) to make sure the light level is above 300 lux at point (3.8, 2.8, 0.8) and 500 lux at point (2.6, 2.3, 0.8) in Figure 6. The occupant works on the PC at the former point and do paperwork at the latter point, therefore the design light level for the former point is lower than the latter. The average annual infiltration rate is 0.47ac/h. There is a bottom hung window on the north façade with a geometry of 0.97m (width) x 0.439m (height) including frames. The horizontal pivot of the window is at the bottom of the opening, and the maximum openable angle is 20°. It introduces natural ventilation to the room when the internal air temperature is above 24°C.
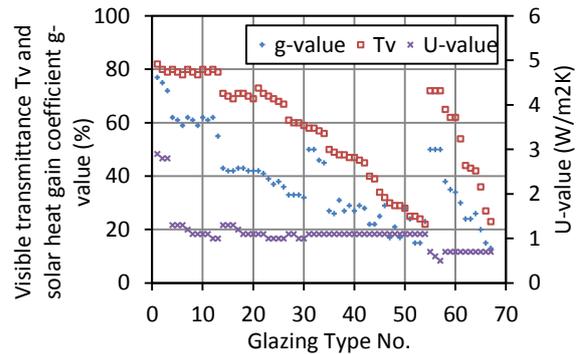

Figure 9 Performance properties for each glazing type.

Table 3 Kingspan Kooltherm K17 insulated dry-lining board data (Kingspan, 2012).

Panel Type	Insulation layer thickness (mm)	Thermal resistance (m^{2}K/W)	Price per board including VAT (£)	Embodied carbon per board (kg CO$_2$ eq/kg)
1	0	0	0.0	0
2	25	1.15	47.3	0.049
3	30	1.35	50.9	0.058
4	35	1.55	54.6	0.067
5	40	1.8	58.2	0.077
6	45	2.2	58.2	0.095
7	50	2.4	58.3	0.103
8	55	2.65	58.9	0.114
9	60	2.9	59.6	0.125
10	65	3.15	60.3	0.135
11	70	3.35	60.9	0.144

- Multi-objective Optimisation

Based on the result of the preliminary investigation, areas of greater improvement potential are identified. A systematic optimisation study was carried out to further explore these areas in search for optimal façade design solutions.

The three design variables are: (i) window-to-wall ratio (*WWR*), (ii) Glazing type *GT* 1-67, (iii) insulation panel type for the opaque wall (*WB*), and (iv)insulation panel type for the floor (*FLB*) (Table 3). *WWR* ranged from 30% to 80%, increasing at an interval of 10%. Glazing type is a discrete variable. For each of the 67 glazing types, three basic thermal performance properties (thermal transmittance *U-value*, solar heat gain coefficient *g-value* and visible transmittance T_v) were specified (Figure 9).

The three optimisation objectives are: (i) to minimise PB_{carbon}; (ii) to minimise PB_{cash}; and (iii) to maximise C_{IEQ}. Since the service life of a façade is 30 years, two constraints are that PB_{carbon} and PB_{cash} should be no more than 30.

A genetic algorithm NSGA-II (Deb *et al.*, 2002) was chosen to perform the optimisation. The original NSGA-II algorithm developed by Kanpur Genetic Algorithm Laboratory (KGAL, 2010) was limited to continuous variables. The MATLAB 7.6 scripts were therefore modified to handle discrete variables. The crossover and mutation probability are 0.9 and 0.1, respectively. The distribution indexes for crossover and mutation are both 20. The population size is 300. The number of generation is 15. The analysis was carried out on a Windows-based PC with a 2.83 GHz processor and 8GB of RAM.

RESULT ANALYSIS AND DISCUSSION

Computational model validation

The experimental and simulated dry bulb temperature for Office A are compared in Figure 10. The good match (R^2-value = 99.7%) between the simulated and measured dry bulb temperature in Location B ensures the boundary condition of the south surface of Office A is simulated correctly.
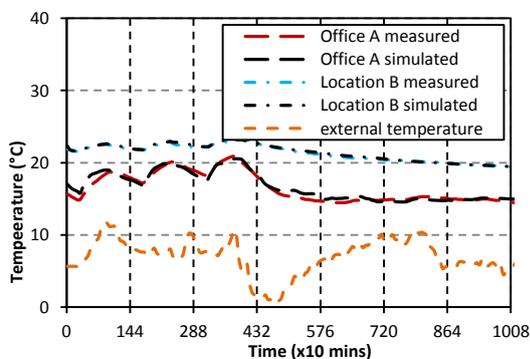

Figure 10 External dry bulb temperature, numerical and experimental dry bulb temperature in Office A.

The simulated dry bulb temperature in Office A generally agrees well with the experimental

measurement with an R^2-value of 97.1%, although the simulated temperature is more responsive to the external conditions than was observed in the in-situ measurements. This discrepancy could be due to: (i) modelling simplifications, e.g., solar radiation is not measured and therefore taken from other sources, and thermal mass in the office was assumed to be equivalent to $3m^3$ wood and might not be perfectly accurate; or (ii) a deficiency of the 'step-function' radiator model in EnergyPlus (Zhai and Chen 2005). Nevertheless, an R^2-value of 97.1% indicates an acceptable level of agreement.

Preliminary investigation

- Environmental value, PB_{carbon}

Table 4 shows the carbon emission, carbon saving, embodied carbon of implementing the strategies, and PB_{carbon} of the five strategies. a short carbon payback period (<1 year) is found for S_G. S_W and S_Fl require mediate carbon payback period. A much longer carbon payback period for S_Fr is mainly due to the high embodied carbon of aluminium frames with thermal break in combination with the relatively smaller amount of energy it saves.

Table 4 CO_2 equivalent emission, CO_2 saving, and carbon payback period of the five strategies.

STRA-TEGY	(1)	(2)	(1)+(2)	(3)	(4)	(5)
S_O	28	426	455	0	0	0
S_W	28	396	424	31	363	11.8
S_G	29	262	291	164	77	0.5
S_Fr	28	404	431	24	576	24.3
S_Fl	28	305	333	122	1090	8.9

(1) Annual CO_2 equivalent emission from consuming electricity (kg CO_2 eq);
(2) Annual kg CO_2 equivalent emission from consuming natural gas (kg CO_2 eq);
(3) Embodied carbon of implementing the improvement (kg CO_2 eq);
(4) Saved carbon (kg CO_2 eq);
(5) CO_2 payback period (year).

Table 5 Economic cost for energy consuming, initial capital cost of implementing the improvement strategies, and the cash payback period.

STRA-TEGY	(1)	(2)	(1)+(2)	(3)	(4)	(5)
S_O	4.0	71.9	76.0	0	0	0
S_W	4.0	66.8	70.9	5.1	182	35
S_G	4.2	44.2	48.4	27.6	935	34
S_Fr	4.0	68.1	72.0	4.0	N/A	N/A
S_Fl	4.0	51.4	55.4	20.6	647	31

(1) Annual economic cost for electricity (£);
(2) Annual economic cost for natural gas (£);
(3) Saved energy cost (£);
(3) Initial capital cost of implementing the improvement the strategies (£);
(4) Cash payback period (year).

- Economic value, PB_{cash}

Table shows the economic cost for energy consuming, initial capital cost of implementing the strategies, and PB_{cash} of the five strategies. S_G

reduces the heating energy demand by 38%, however, due to the relatively high initial capital cost of glazing, the cash payback period is still very long. S_Fl reduces the heating energy demand by 28%, but the initial capital cost is high which results a long cash payback period. S_W has a low initial capital cost, but since the saving is limited, the cash payback period is also quite long.

- Social value, C_{IEQ}

Table 4 shows the PPD and C_{IEQ} of the five strategies. S_Fl and S_G produce more improvement in occupant's thermal comfort compared to S_W and S_Fr. Accordingly, C_{IEQ} for S_G and S_Fl are much lower.

Table 4 PPD and IEQ cost

STRATEGY	PPD (%)	C_{IEQ} (k£)
S_O	15.2	891
S_W	14.8	805
S_G	13.7	640
S_FR	14.8	813
S_FL	14.0	649

The comparison of the three design objectives shows that S_G and S_Fl generally have larger potential to make an improvement. S_W is less beneficial due to the relatively small area of the opaque wall. S_Fr reduces the heating energy demand, but the largest drawback is the high embodied carbon. Nevertheless, the frame system will need to be replaced to accommodate the new insulated glazing units.

Multi-objective optimisation

It is assumed that all possible façade systems adopt the framing system described in strategy S_Fr. The cost of the framing system is ignored in the calculation due to lack of information. When the simulated WWR is smaller than the existing WWR (67.5%), the shortfall in opaque wall area is composed of 6mm opaque glazing, 110mm rockwool and 114.3mm. The cost of this opaque composite wall is assumed to be £190/m^2.
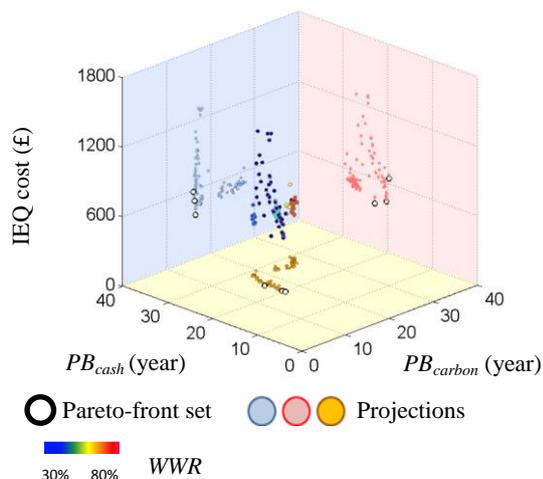

Figure 11 Optimisation result.

The computational time for this analysis was 4.5 hours. Figure 11 shows the possible solutions that

have been visited by the multi-objective optimisation algorithm.

Table lists the solutions on the Pareto-fronts. Glazing types of low U-values are required in the optimal solutions. In order to achieve a good comfort level, slightly lower g-value (less beneficial solar heat gain in winter) can be compensated by reduced U-value (better insulation). In order to achieve the optimal balance between PB_{Carbon} and PB_{Cash}, PB_{Carbon} and C_{IEQ}, or PB_{cash} and C_{IEQ}, a small WWR is necessary. None of the candidates represent the optimal trade-offs among all the design objectives. Therefore, sacrifices of some design objectives have to be made in order to determine the final solution.

Table 7 The optimal façade solution.

GT	WWR (%)	FLB	WB	PB_{Carbon} (year)	PB_{Cash} (year)	C_{IEQ} (k£)
Current	67.5	1	1	0	0	987
Optimal trade-offs between PB_{Carbon} and PB_{Cash}						
13	30	9	3	**16.2**	**20.4**	503
18	30	11	1	**16.4**	**19.8**	639
57	30	2	6	**15.9**	**24.0**	584
Optimal trade-offs between PB_{Carbon} and C_{IEQ}						
13	30	9	3	**16.2**	20.4	**503**
57	30	11	8	**16.4**	23.0	**380**
57	30	2	6	**15.9**	24.0	**584**
Optimal trade-offs between PB_{Cash} and C_{IEQ}						
12	30	11	11	16.6	**20.4**	**434**
18	30	11	1	16.4	**19.8**	**639**
57	30	11	8	16.4	**23.0**	**380**

If larger WWRs are preferable ($WWR \geq 50$), the optimal solution are shown in **Error! Reference source not found.**. The one marked with '*' is recommended, because it represents the optimal trade-offs between the three design objectives.

Table 8 The optimal façade solution, if WWR≥50%.

GT	WWR (%)	FLB	WB	PB_{Carbon} (year)	PB_{Cash} (year)	C_{IEQ} (k£)
Current	67.5	1	1	0	0	987
Optimal trade-offs between PB_{Carbon} and PB_{Cash}						
10*	50	11	9	**22.3**	**27.2**	442
12	70	9	7	**24.8**	**26.3**	461
13	60	7	8	**23.4**	**26.5**	452
13	60	8	11	**23.5**	**26.4**	444
Optimal trade-offs between PB_{Carbon} and C_{IEQ}						
10*	50	11	9	**22.3**	27.2	**442**
Optimal trade-offs between PB_{Cash} and C_{IEQ}						
10*	50	11	9	22.3	**27.2**	**442**
12	70	9	7	24.8	**26.3**	**461**
13	70	11	5	25.1	**26.4**	**444**

CONCLUSION

The paper described how a whole-life, value-based approach was used to identify optimal façade solutions for a refurbishment project. In-situ measurement was implemented to provide reliable data as the basis for validating the building energy simulation model. Preliminary investigation found a

preliminary investigation found that S_G and S_Fl offer a larger potential to improve the value of the office than S_Fr and S_W. Multi-objective optimisation was performed to further explore these strategies. The results show that more insulation and high to moderate *g*-value of glazing is required. A low *WWR* is required. The favoured option is a façade with higher *g*-value to transmit more beneficial solar heat gain in winter. The optimal strategies greatly improves the occupant comfort.

NOMENCLATURE

PPD,	Predicted percentage of dissatisfied (%);
w_h,	Weight of the occupancy in Hour *h*;
IEA,	Acceptance of indoor environmental quality (%);
IEQ,	Satisfaction of indoor environmental quality;
ζ_2,	The CO_2 concentration (ppm);
ζ_3,	The equivalent noise level (dBA);
ζ_4,	The illumination (lux) at working plane;
φ_1,	The acceptance of thermal comfort (%);
φ_2,	The acceptance of air quality (%);
φ_3,	The acceptance of aural comfort (%);
φ_4,	The acceptance of light level (%);
k_1,	The relative importance of thermal comfort;
k_2,	The relative importance of air quality;
k_3,	The relative importance of aural comfort;
k_4,	The relative importance of light level;
WWR,	Window-to-wall ratio (%);
GT,	Glazing Type No.;
t_i,	Thickness of insulation attached to the floor;
PB_{cash},	Cash payback period (year);
PB_{carbon},	Carbon payback period (year);
OP,	Occupant productivity (%).

ACKNOWLEDGEMENT

REFERENCES

AEA Ltd. 2011. Guidelines to Defra / DECC's GHG Conversion Factors for Company Reporting.

ASHRAE. 2011. "ASHRAE International Weather for Energy Calculations (IWEC) data." , available from http://apps1.eere.energy.gov/buildings/energyplus/cfm/weather_data3.cfm/region=6_europe_wmo_region_6/country=GBR/cname=United Kingdom. assessed on 20th October 2010.

ASHRAE. 2009, ASHRAE Handbook - Fundamentals, Atlanta, USA.

Chartered Institution of Building Services Engineers. 2006. CIBSE Guide A: Environmental design. London, UK.

Deb, K., Pratap, A., Agarwal, S., Meyarivan, T. 2002. "A Fast and Elitist Multiobjective Genetic Algorithm: NSGA II." IEEE Transactions on Evolutionary Computation 6(2): 182-197.

Digital technology group, Computer laboratory, University of Cambridge. "Digital technology group cambridge weather station." Available on http://www.cl.cam.ac.uk/research/dtg/weather/ accessed on 19th January, 2012.

Duska, M., Lukes, J., Bartak, M., Drkal, F., Hensen, J. 2007. "Trend in heat gains from office equipment." In proceedings of the 6th international conference on Indoor Climate of Buildings, Strbske Pleso, Bratislava.

Department for Communities and Local Government. 2010. "Building Regulations for England and Wales 2000 Part L2A". UK.

Hammond, G., and Crai, J. 2008. Inventory of carbon & energy (ICE). Bath, UK.

Jin, Q., Overend, M. and Thompson P. 2012. "Towards productivity indicators for performance-based façade design in commercial buildings." Building and Environment 57:271-281.

Kellenberger, D., Nicolas, P., and Scion. 2008. Technology *LCA-based Windows Calculator*.

Kanpur Genetic Algorithm Labaratory. 2010. Available on http://www.iitk.ac.in/kangal/. assessed on 15th Oct, 2010.

Laurance Berkeley National Lab. 2011. "EnergyPlus."

Micronics Ltd. 2010. Portaflow 330 Technical Datasheet. Issue 3.3. Bucks, UK.

Kingspan, "Kingspan K17 board information." Available on http://www.kingspaninsulation.co.uk/Products/Kooltherm/Kooltherm-K17-Insulated-Plasterboard/Overview.aspx assessed on 20th Apr, 2012.

Schuco Ltd. 2012. available on http://www.schueco.com/web/uk. accessed on 12th March, 2012.

Thompson, P. 2011. Personal correspondence.

Yeniay, O. 2005. "Penalty function methods for constrained optimisation with genetic algorithms." Mathematical and computational applications 10 (1): 45-56.

Zhai, Z. J., Chen, Q. Y. 2005. "Performance of coupled building energy and CFD simulations." Energy and Buildings 37: 333-344.